

Electronic Supplementary Information

Sub-10 nm metal-dispersed crystalline C₃N₅ for photocatalytic CO₂ reduction to produce formic acid and acetic acid

Sue-Faye Ng,^{a,b} Bifang Li,^c Joel Jie Foo,^{a,b} Xianhai Zeng,^d Sibowang,^{c,} Wee-Jun Ong^{a,b,e,f,g,h,*}*

^a School of Energy and Chemical Engineering, Xiamen University Malaysia, Selangor Darul Ehsan 43900, Malaysia.

^b Center of Excellence for NaNo Energy & Catalysis Technology (CONNECT), Xiamen University Malaysia, Selangor Darul Ehsan 43900, Malaysia.

^c State Key Laboratory of Photocatalysis on Energy and Environment, College of Chemistry, Fuzhou University, Fuzhou, Fujian, China.

^d College of Energy, State Key Laboratory of Physical Chemistry of Solid Surfaces, Xiamen University, Xiamen 361102, China.

^e State Key Laboratory of Physical Chemistry of Solid Surfaces, College of Chemistry and Chemical Engineering, Xiamen University, Xiamen 361005, China.

^f Gulei Innovation Institute, Xiamen University, Zhangzhou 363200, China.

^g Shenzhen Research Institute of Xiamen University, Shenzhen 518057, China.

^h Department of Chemical and Biological Engineering, College of Engineering, Korea University, 145 Anam-ro, Seongbuk-gu, Seoul, 02841 Republic of Korea.

*Corresponding author

Sibowang: Email: sibowang@fzu.edu.cn

Wee-Jun Ong: Email: weejun.ong@xmu.edu.my; connect.coe@xmu.edu.my

Methodology

Chemicals

3-amino-1,2,4-triazole (3AT; $\geq 95\%$) and potassium chloride (KCl; ACS reagent, 99.0-100.5%) were obtained from Sigma Aldrich. Lithium chloride (LiCl; $\geq 98.5\%$) was obtained from Thermo Scientific. Nafion D-521 dispersion, 5% w/w in water was purchased from Alfa Aesar. Metal precursors used were silver nitrate (AgNO_3 ; Fisher Scientific, $\geq 99.9\%$), bismuth (III) nitrate pentahydrate ($\text{Bi}(\text{NO}_3)_3 \cdot 5\text{H}_2\text{O}$; Acros), magnesium nitrate hexahydrate ($\text{Mg}(\text{NO}_3)_2 \cdot 6\text{H}_2\text{O}$, Alfa), and tungsten (VI) chloride (WCl_6 , Thermo Scientific). Iron (III) nitrate nonahydrate ($\text{Fe}(\text{NO}_3)_3 \cdot 9\text{H}_2\text{O}$, Fisher Scientific), potassium iodide (KI, Merck, $\geq 99.5\%$), and tert-butanol (TBA, Lab Serv), terephthalic acid (Merck) and triethanolamine (TEOA, Chemiz) were used for scavenger tests and as a sacrificial agent. All aqueous solutions were prepared with deionized (DI) water ($> 18.2 \text{ M}\Omega \cdot \text{cm}$ resistivity).

Synthesis of CCN

Crystalline C_3N_5 (CCN) was synthesized based on our previous work.¹ Firstly, 4 g of 3AT, 12.96 g of LiCl and 10.92 g of KCl were ground in a pestle mortar for 5 min and then transferred into a porcelain crucible. This was then heat up in a chamber furnace at 500 °C for 4 h at a ramping rate of 12 °C min^{-1} . The resulting powder was washed with warm DI water (70 °C) and filtered. The resulting powder after drying in an oven at 80 °C overnight was labelled as CCN.

Synthesis of metal dispersed CCN

100 mg of CCN was sonicated in a 100 mL aqueous solution of 10 vol% TEOA for 1 h. Then, a set amount of 10 mg mL^{-1} AgNO_3 was added into the CCN solution dropwise with a micropipette based on a calculated weight percent of 1.5. This was transferred into a double-walled reactor attached to a circulating bath set to 20°C . The reactor was purged with N_2 gas for 30 min in the dark before being illuminated with a 300 W Xe lamp (PF300-T8 300W, CEALIGHT) with an AM1.5 light filter for 30 min. The resulting solution was filtered and vacuum dried at 60°C overnight and labelled as Ag1.5. For Bi, Mg and W with weight loading percentage 1.5 wt%, the same procedure was used but with $\text{Bi}(\text{NO}_3)_3 \cdot 5\text{H}_2\text{O}$, $\text{Mg}(\text{NO}_3)_2 \cdot 6\text{H}_2\text{O}$, and WCl_6 solution instead of AgNO_3 . The procedure for Ag1.5 was also used for preparing other sample compositions (Ag0.5, Ag3, and Ag5), but with the calculated weight percent changed to 0.5, 3, and 5 wt%, respectively.

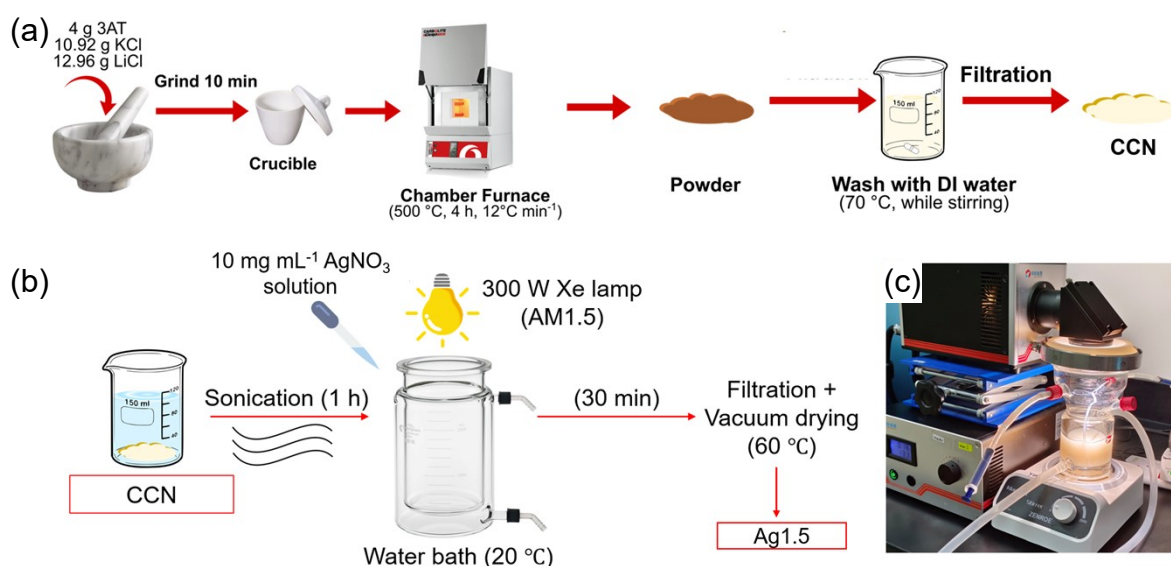


Fig. S1. Synthesis steps for (a) CCN and (b) Ag1.5. (c) Setup for the photodeposition process to prepare metal-dispersed CCN.

Materials characterization

Low- and high-resolution transmission electron microscopy (TEM/HRTEM) and selected area electron diffraction (SAED) was conducted on FEI TECNAI G2 F20 X-TWIN with Gatan Orius SC 1000B camera operated at 200 keV equipped with Energy Dispersive X-ray Spectroscopy system (EDS) (Oxford X-MaxN 80T). The crystalline phases of the carbon nitrides were analyzed by powder X-ray diffraction (XRD) with a $\text{Cu K}\alpha$ radiation source at a step size of 0.02° from 5° to 80° (Panalytical X'Pert Pro). The elemental composition of the

samples was studied with X-ray photoelectron spectroscopy (XPS) (Kratos AXIS Ultra DLD). The ultraviolet-visible diffuse reflectance spectroscopy (UV-vis DRS) was recorded with a Shimadzu RF-6000 UV-vis spectrophotometer ($200 < \lambda < 800$ nm). The Fourier transform infrared (FTIR) spectra were obtained by infrared spectrometer (PerkinElmer Spectrum Frontier), using a standard ATR technique. The photoluminescence (PL) spectra were acquired on Shimadzu RF-6000 Spectrofluorometer. The elemental composition of samples was obtained through PerkinElmer ICP-OES Optima 8000 and X-ray photoelectron spectroscopy (ESCALAB 250, Thermo-VG Scientific S). *In situ* diffuse reflectance infrared Fourier transform spectroscopy (DRIFTS) measurements were obtained with a Thermo Scientific Nicolet iS50-FTIR spectrometer with a MCT detector and a reaction cell. 30 mg of the sample was added alongside a drop of deionized water on the center of the reaction cell before purging with N₂ gas (20 mL min⁻¹). Then, CO₂ gas was introduced before light illumination (300 W Xe lamp, $\lambda > 400$ nm). The time-resolved fluorescence emission spectra were recorded with a Deltapro Fluorescence Lifetime System. Atomic Force Microscopy (AFM) and Kelvin Probe Force Microscopy (KPFM) was performed on a Park Systems (NX10) system using a superluminescent diode (SLD) cantilever beam. The light source used for KPFM was 600 nm wavelength.

Photocatalytic performance measurements

The solar-driven CO₂ reduction reaction (CO₂RR) was carried out in a quartz glass reactor with a water circulating bath set to 20 °C. The photocatalysts (20 mg) were first dispersed in a 20 mL aqueous solution with acetonitrile:water at a 4:1 volume ratio, 1 vol% of TEOA, 2 mg of CoCl₂•6H₂O and 64 mg of bipyridine. The system was then purged for 30 min with CO₂ gas in the dark to remove residual air. After which, the light source (300 W Xe lamp; CEAULIGHT, PF300-T8 300W) equipped with a 400 nm cutoff filter was switched on. The light intensity was measured to be 100 mW cm⁻² at the distance between the light source and the sample. Gas chromatography (Agilent GC 8890, Helium carrier gas) was used to measure the gaseous product (CO, O₂) during the reaction. The Agilent 1260 Infinity liquid chromatography (HPLC) system (Agilent InfinityLab Poroshell 120 EC-C18; 25 °C; 2.5 μL; flow rate: 0.4 mL min⁻¹; mobile phase: 0.01 vol% H₃PO₄/acetonitrile=80:20) was used to quantify the liquid products. The error bars were obtained by repeating the tests in triplicate. The calibration curve for FA and AA can be found below.

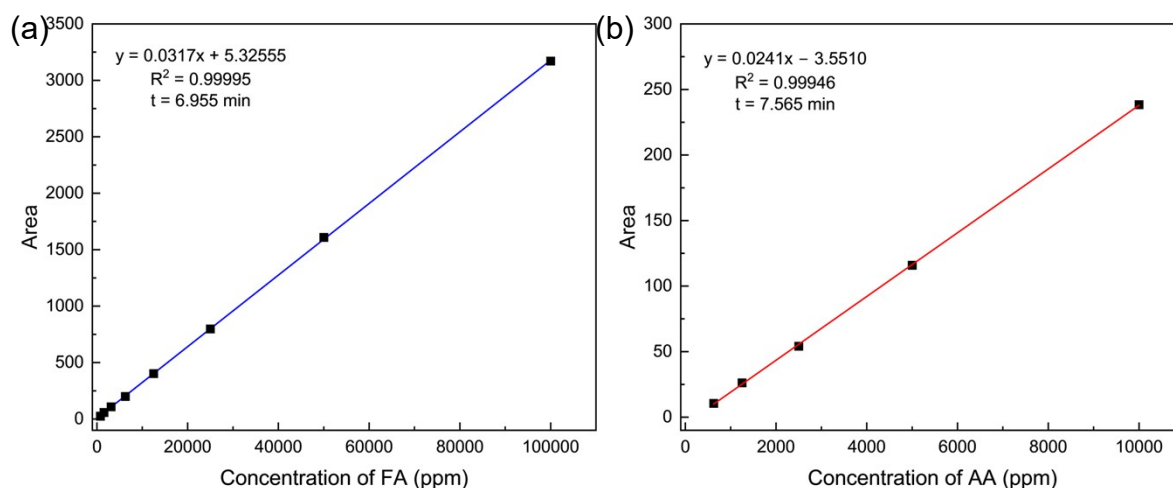


Fig. S2. Calibration curves for (a) FA and (b) AA.

The terephthalic acid test for $\bullet\text{OH}$ radicals was conducted with the same conditions as the photocatalytic CO_2RR test but substituting TEOA with terephthalic acid in the same molar amount. The supernatant was collected after 1 h light irradiation by passing the reaction solution through a $0.2\ \mu\text{m}$ syringe filter. The terephthalic acid reacts with the as-produced $\bullet\text{OH}$ under light illumination to form 2-hydroxyterephthalic acid, which was detected using PL at 425 nm.

Apparent quantum efficiency (AQE) measurements for CO and FA were conducted with different band-pass wavelength irradiations (i.e. 380, 400, 420, 450, and 500 nm). The light intensity was recorded from a spectroradiometer (CEAULIGHT, CEL-NP2000). The AQE value for CO and FA was calculated with the following formula.

$$AQE = \frac{2 \times \text{number of evolved CO or FA molecules}}{\text{Number of incident photons}} \times 100\% \quad (1)$$

Photoelectrochemical measurements

The Metrohm Autolab (PGSTAT204) electrochemical workstation with a standard three-electrode cell was used for photoelectrochemical measurements. The counter electrode and reference electrode used were a Pt sheet and Ag/AgCl (in 3.0 M KCl), respectively. The electrolyte was a 0.1 M Na₂SO₄ solution. For the working electrode, 5 mg of the catalyst, 40 μ L of Nafion and 200 μ L of absolute ethanol were used as the catalyst ink and stirred overnight. After which, 25 μ L of the solution was drop casted onto a fluorine-doped tin oxide (FTO) glass (1×1 cm²) and left to dry at room temperature. Electrochemical impedance spectroscopy was conducted at the frequency range of 0.01 to 10⁵ Hz with an amplitude of 10 mV. Transient photocurrent was conducted at a potential of 0.5 V vs. Ag/AgCl with the light (300 W CEAULIGHT Xenon lamp, PF300-T8 300W) on and off at 30 s intervals. The AM1.5 filter was used if unstated, and 420, 450, 500, 550 nm bandpass filter was used for the transient photocurrent tests with varying wavelengths at a light intensity of 100 mW cm⁻². Linear sweep voltammetry was obtained from -1.0 V to 0 V vs. Ag/AgCl at a scan rate of 0.01 V s⁻¹. Mott-Schottky was measured from the voltage range of -1.25 to 0.6 V at the frequencies of 250, 500, 750 and 1000 Hz. Equation 2 was used to determine the lifetime of injected electrons (τ) for the catalysts:

$$\tau = 0.5\pi F_p \quad (2)$$

Whereby F_p = inverse minimum frequency². A 300 W Xe lamp equipped with AM1.5 filter was used for the transient photocurrent test (0.5 V vs. Ag/AgCl).

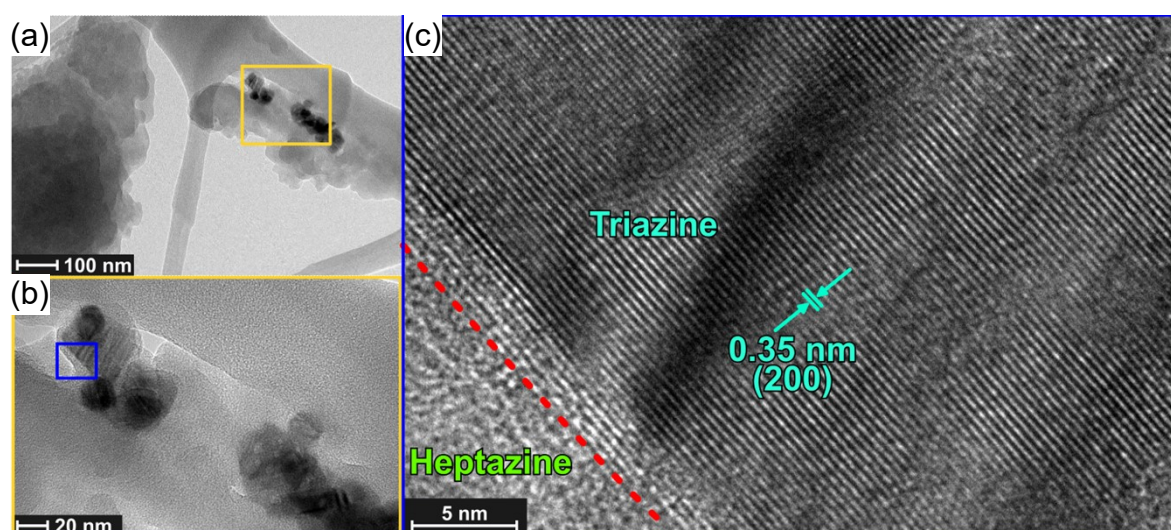


Fig. S3. (a-b) TEM and (c) HRTEM images of pristine CCN.

Table S1. Peak location and full-width half maximum of CCN and Ag-CCN with varying weight loadings.

Catalyst	2 θ (degree) [FWHM]						
CCN	12.15 ^b [1.30]	21.13 ^b [1.13]	26.91 ^b [2.14]	27.78 ^a [0.60]	29.11 ^b [1.56]	32.35 ^b [1.27]	-
Ag0.5	12.07 ^b [1.333]	21.08 ^b [1.30]	26.66 ^b [0.81]	27.03 ^a [2.15]	28.78 ^b [2.52]	32.24 ^b [1.52]	38.26 [0.001]
Ag1.5	12.18 ^b [1.08]	21.15 ^b [0.88]	26.64 ^b [1.23]	27.68 ^a [1.55]	29.23 ^b [1.09]	32.32 ^b [0.79]	38.37 [0.90]
Ag3	12.07 ^b [1.19]	21.21 ^b [1.00]	26.66 ^b [1.61]	27.65 ^a [1.19]	29.16 ^b [1.27]	32.36 ^b [0.73]	38.20 [1.80]
Ag5	12.04 ^b [1.46]	21.08 ^b [0.17]	26.70 ^b [1.40]	27.40 ^a [2.10]	29.22 ^b [1.20]	32.27 ^b [0.09]	38.23 [1.56]

^a Heptazine peak

^b Triazine peak

Table S2. Chemical compositions of CCN and Ag1.5 samples obtained from XPS.

Catalyst	Element (atm%) [wt%]					
	C	N	O	K	Cl	Ag
CCN	38.39 [32.23]	39.87 [39.03]	18.68 [20.89]	1 [2.73]	2.06 [5.11]	-
Ag1.5	33.95 [27.97]	30.62 [29.42]	34.18 [38.5]	0.58 [1.55]	0.28 [0.58]	0.39 [2.9]

Table S3. AQE values of Ag1.5 using different band-pass filters.

Wavelength (nm)	380	400	420	450	500
CO produced (μmol)	19	31	11.6	5.4	5.2
FA produced (μmol)	41	80	71	8	5.4
Light intensity (mW)	21.42	103.19	93.62	46.8	38.23
AQE CO (%)	3.90	1.25	0.49	0.43	0.45
AQE FA (%)	8.37	3.20	3.00	0.43	0.70

Table S4. Literature comparison of photocatalytic CO₂RR performance for different carbon nitride-based catalysts.

Catalyst	Light source	Reactant medium	Production (μmol h ⁻¹)	AQE (%)	Ref.
N-defect g-C ₃ N ₄	300 W Xe lamp	20 mg catalyst MeCN/TEOA=4:1	CO: 226.1 CH ₄ : 4	-	3
Ultrathin g-C ₃ N ₄	300 W Xe lamp (400 nm)	5 mg catalyst MeCN/TEOA=2:1	CO: 13.7	-	4
P-Cu doped g-C ₃ N ₄	300 W Xe lamp	0.5 mg catalyst MeCN/TEOA=25:3	Et: 616.6	12.55 ^a [350 nm]	5
O-doped boron nitride	300 W Xe lamp (320 < λ < 780 nm)	10 mg catalyst MeCN/TEOA=3:1	CO: 32	-	6
TiO-CN	300 W Xe lamp (420 nm)	3 mg catalyst MeCN/TEOA=3:1 CoCl ₂ •6H ₂ O: 0.25 μmol Bipyridine: 15 mg	CO: 283.9 H ₂ : 36.5	-	7
Ru-complex modified g-C ₃ N ₄	300 W Xe lamp (400 nm)	8 mg catalyst MeCN/TEOA=4:1	FA: 1.854	-	8
Ru/Ag/plasma g-C ₃ N ₄	410 and 460 nm- centered LEDs	4 mg catalyst DMA/TEOA= 4:1	FA: 6.4 CO: 0 H ₂ : 0.08	1.6 ^b [400 nm]	9
Trimesic acid modified g-C ₃ N ₄	300 W Xe lamp (400 nm)	30 mg catalyst MeCN/TEOA= 7:1 CoCl ₂ •6H ₂ O: 1 μmol Bipyridine: 15 mg	CO: 30.19 H ₂ : 7.32	-	10
Ag1.5	300 W Xe lamp (400 nm)	20 mg catalyst MeCN/H ₂ O =4:1 TEOA= 1 vol% CoCl ₂ •6H ₂ O: 2 mg Bipyridine: 64 mg	CO: 404 FA: 1296 AA: 390	3.2 ^b [400 nm]	This work

TEOA: Triethanolamine; MeCN: Acetonitrile; DMA: *N,N*-dimethylacetamide; FA: formic acid; AA: acetic acid; Et: ethane; ^a: AQE value for ethane; ^b: AQE value for formic acid.

Table S5. Charge transfer resistance of CCN and Ag1.5 obtained from EIS curve fitting.

Sample	Rp.R (kΩ·cm ⁻²)
CCN	1090
Ag1.5	113

Table S6. Average emission lifetime (τ_{ave}), fastest (τ_1), fast (τ_2) and slow decay component (τ_3) calculated from time-resolved photoluminescence (TRPL) decay spectra

Sample	τ_1 (ns)	τ_2 (ns)	τ_3 (ns)	τ_{ave} (ns)
CCN	3.187873	1.43E+01	0.836	2.14305
Ag1.5	0.0979699	0.8067	0.732742	1.98749

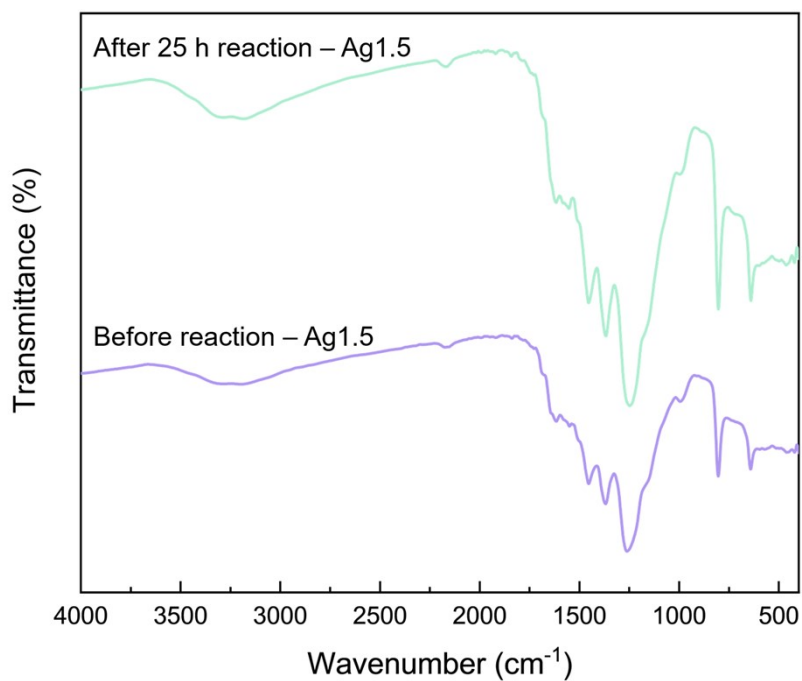


Fig. S4. FTIR spectra of the optimal Ag1.5 catalyst before and after 25 h photocatalytic CO₂RR.

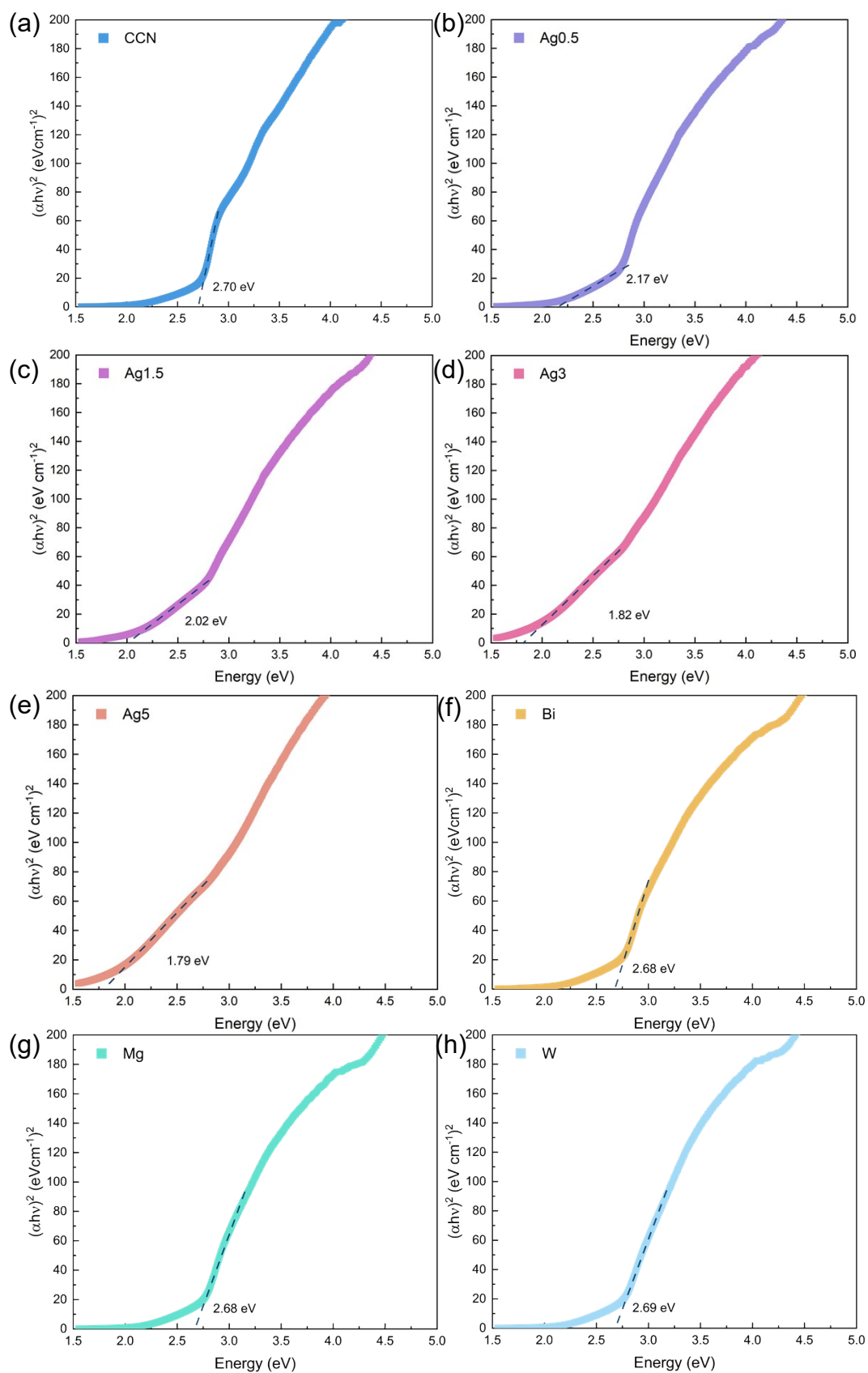


Fig. S5. Tauc plots for (a) CCN, (b) Ag0.5, (c) Ag1.5, (d) Ag3, (e) Ag5, (f) Bi, (g) Mg, and (h) W.

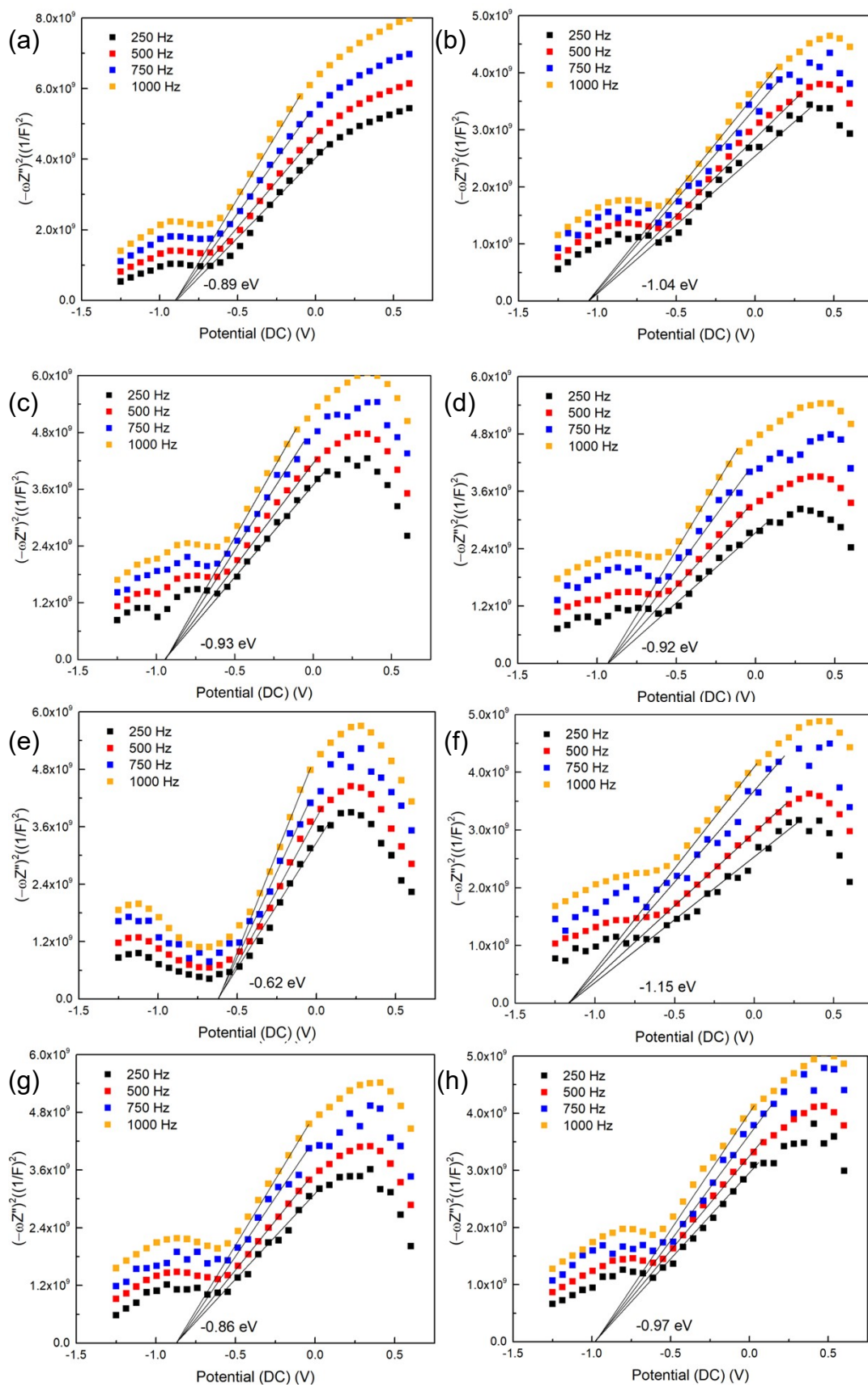


Fig. S6. Mott Schottky plots for (a) CCN, (b) Ag_{0.5}, (c) Ag_{1.5}, (d) Ag₃, (e) Ag₅, (f) Bi, (g) Mg, and (h) W.

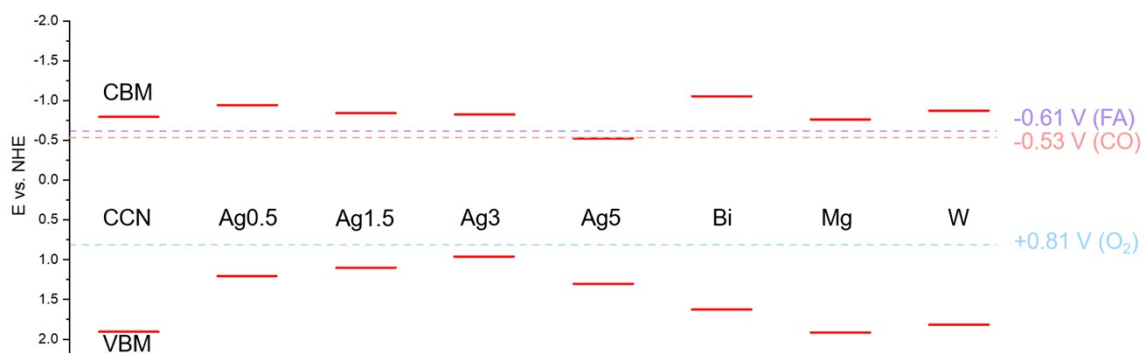


Fig. S7. Band structures of carbon nitride-based catalysts. (CBM: conduction band minimum; VBM: valence band maximum)

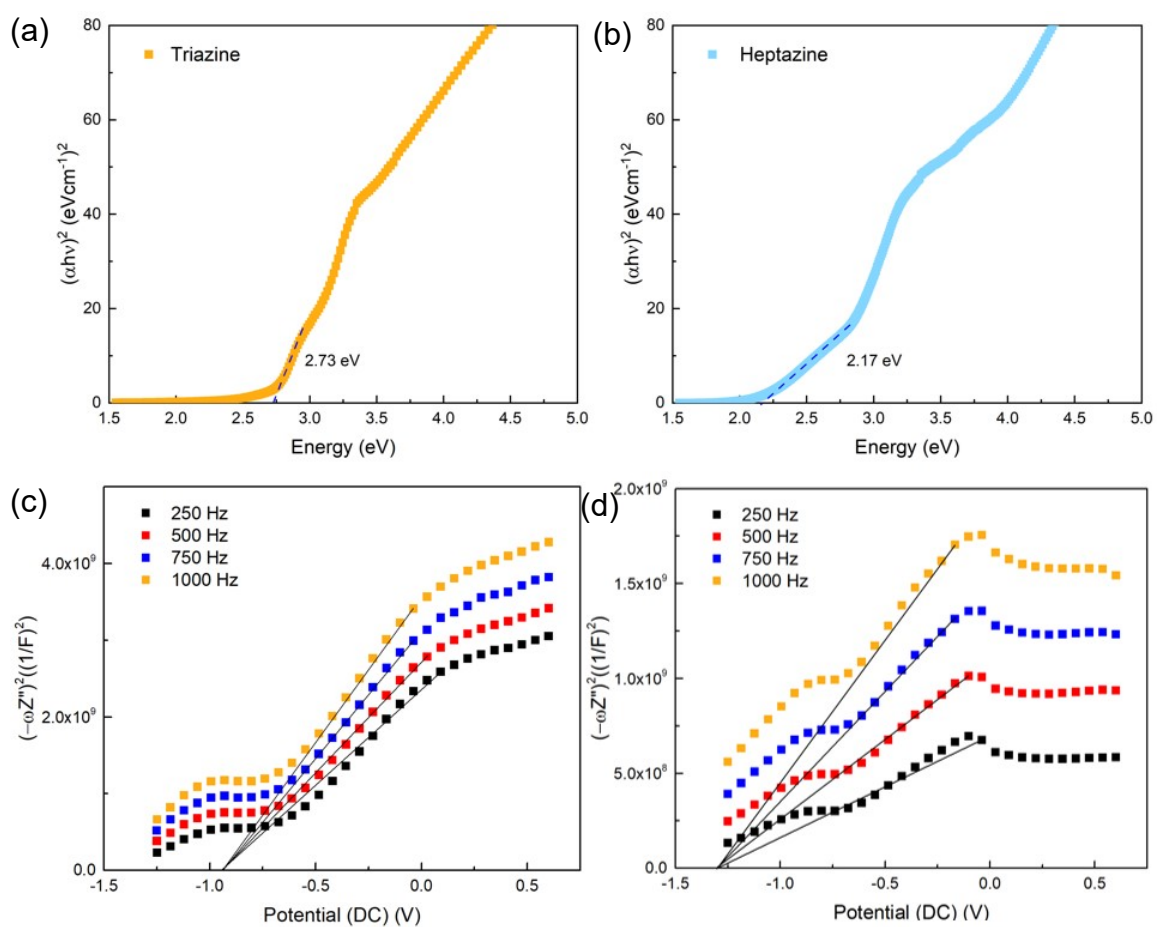


Fig. S8. Tauc plot of triazine and heptazine phase of CCN.

Table S7. Bandgap, conduction band (CB), and valence band (VB) of CCN and metal-dispersed catalysts calculated from Tauc plots and Mott Schottky plots.

Catalyst	Band gap (E_g) (eV)	CB (V vs. NHE)	VB (V vs. NHE)
CCN	2.70	-0.793	1.907
Ag0.5	2.17	-0.943	1.227
Ag1.5	2.02	-0.842	1.178
Ag3	1.82	-0.823	0.997
Ag5	1.79	-0.523	1.267
Bi	2.68	-1.053	1.627
Mg	2.68	-0.763	1.917
W	2.69	-0.873	1.817

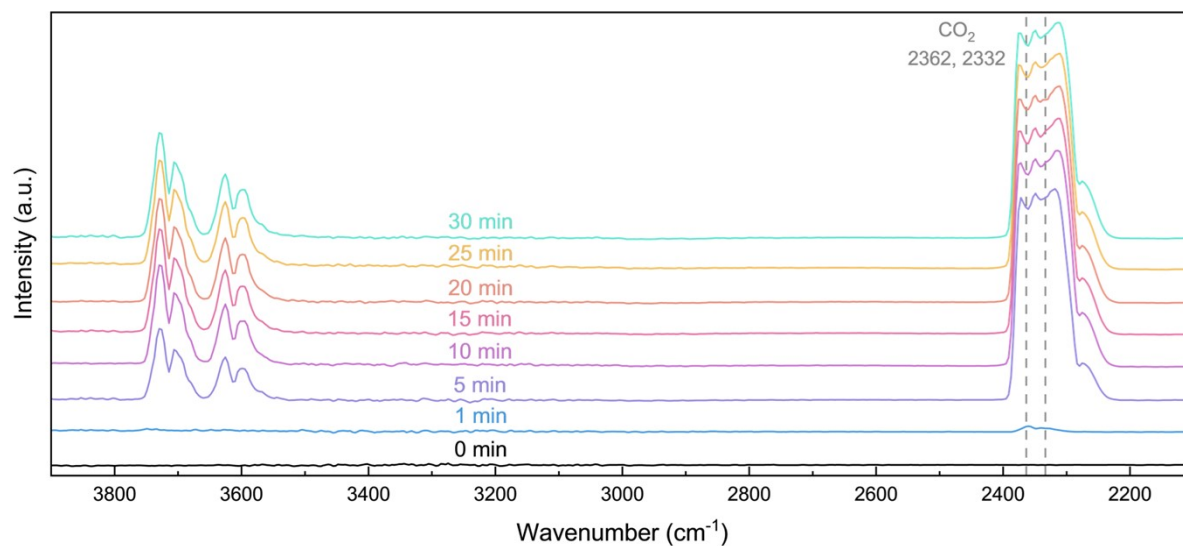


Fig. S9. *In-situ* DRIFTS spectra of Ag1.5 sample in the dark.

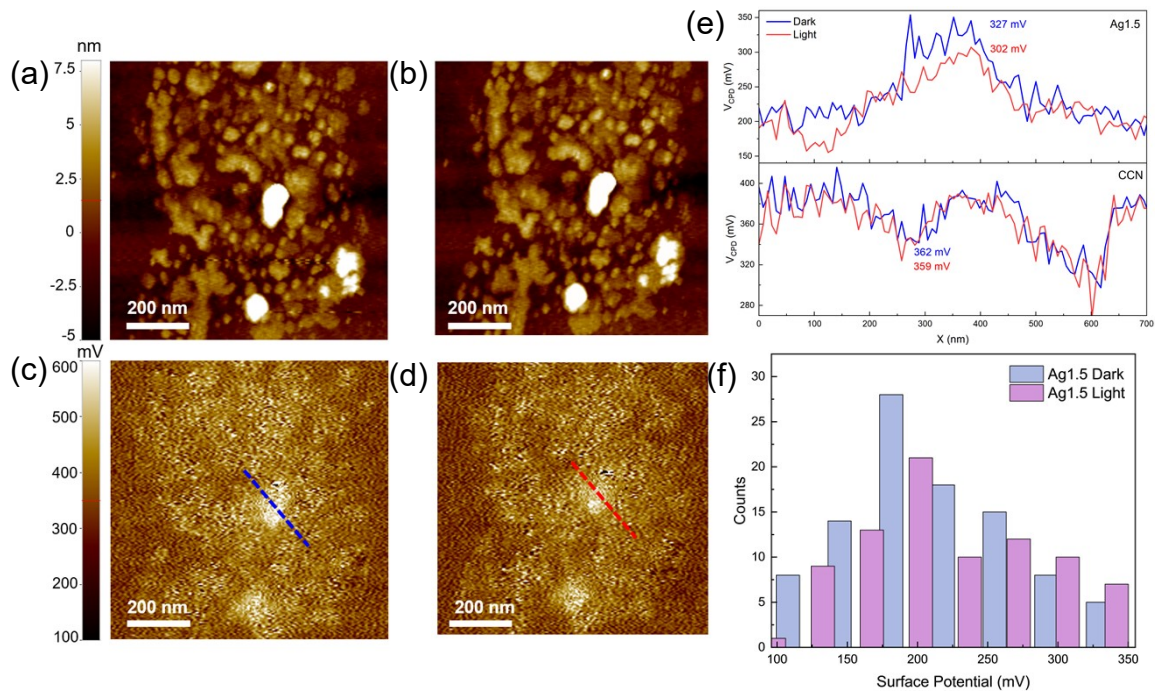


Fig. S10. Atomic force microscopy (AFM) and KPFM surface potential images of Ag1.5 in the (a and c) dark and (b and d) under 600 nm light illumination. (e) Contact potential difference (V_{CPD}) of Ag1.5 and CCN in the dark measured from the blue and red lines (c and d) using KPFM. (f) Histogram of surface potential counts for Ag1.5 in dark and light conditions.

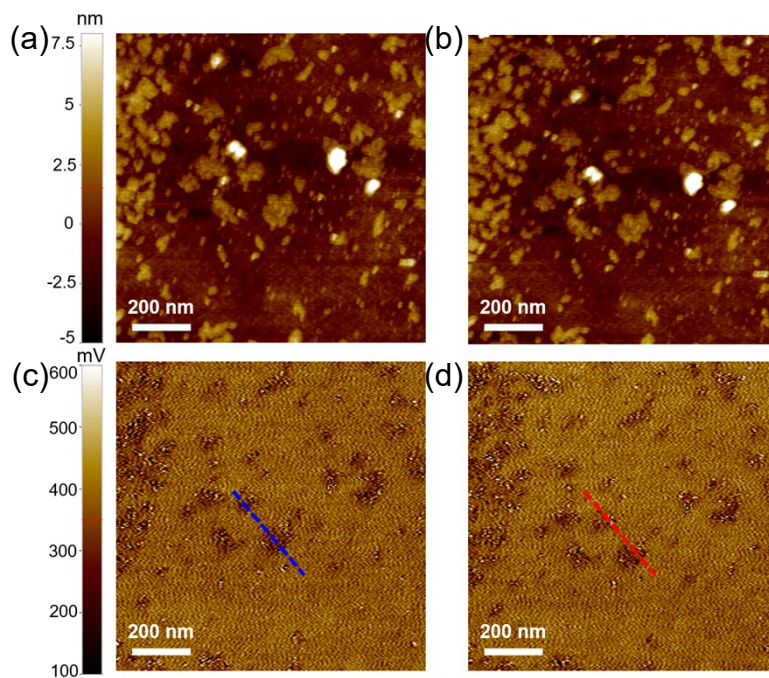


Fig. S11. Atomic force microscopy (AFM) and KPFM surface potential images of CCN in the (a and c) dark and (b and d) under 600 nm light illumination.

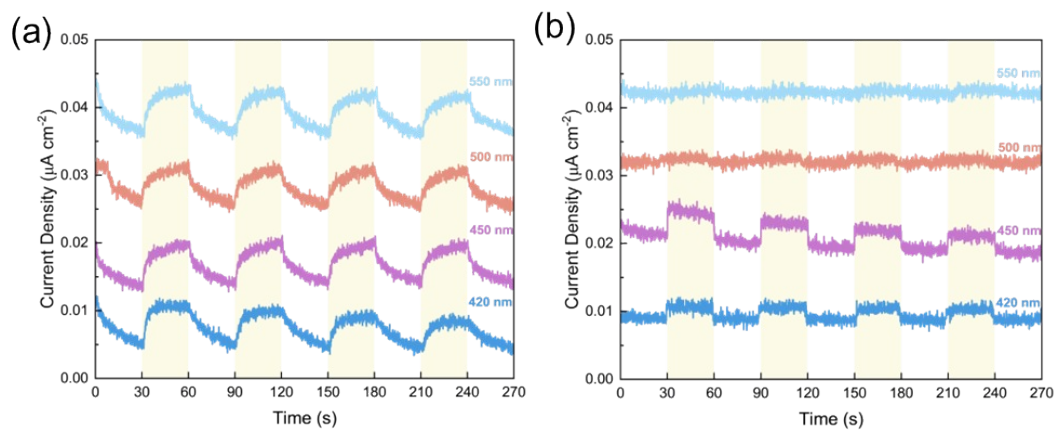


Fig. S12. Transient photocurrent response (a) comparing Ag1.5 and CCN and (b) Ag1.5 using various bandpass filters.

References

1. S.-F. Ng, J. J. Foo and W.-J. Ong, *Mater. Horiz.*, 2024, **11**, 408-418.
2. C. Liu, H. Huang, X. Du, T. Zhang, N. Tian, Y. Guo and Y. Zhang, *J. Phys. Chem. C*, 2015, **119**, 17156-17165.
3. J. Hou, M. Yang, Q. Dou, Q. Chen, X. Wang, C. Hu and R. Paul, *Chem. Eng. J.*, 2022, **450**, 138425.
4. J. Li, C. He, J. Wang, X. Gu, Z. Zhang, H. Li, M. Li, L. Wang, S. Wu and J. Zhang, *Green Chem.*, 2023, **25**, 8826-8837.
5. G. Wang, Z. Chen, T. Wang, D. Wang and J. Mao, *Angew. Chem. Int. Ed.*, 2022, **61**, e202210789.
6. J. Liang, H. Zhang, Q. Song, Z. Liu, J. Xia, B. Yan, X. Meng, Z. Jiang, X. W. Lou and C.-S. Lee, *Adv. Mater.*, 2024, **36**, 2303287.
7. S. Tang, X. Yin, G. Wang, X. Lu and T. Lu, *Nano Res.*, 2019, **12**, 457-462.
8. K. Maeda, R. Kuriki, M. Zhang, X. Wang and O. Ishitani, *J. Mater. Chem. A*, 2014, **2**, 15146-15151.
9. N. Sakakibara, M. Shizuno, T. Kanazawa, K. Kato, A. Yamakata, S. Nozawa, T. Ito, K. Terashima, K. Maeda, Y. Tamaki and O. Ishitani, *ACS Appl. Mater. Interfaces*, 2023, **15**, 13205-13218.
10. A. Hayat, J. Khan, M. U. Rahman, S. B. Mane, W. U. Khan, M. Sohail, N. U. Rahman, N. Shaishta, Z. Chi and M. Wu, *J. Colloid Interface Sci.*, 2019, **548**, 197-205.